JOURNAL OF APPLIED ELECTROCHEMISTRY 8 (1978) 427–436

A quantitative study of shape change in zinc secondary electrodes

S.-P. POA, C. H. WU

Department of Industrial Chemistry, National Tsing Hua University, Hsin-Chu, Taiwan, ROC

Received 24 October 1977

Zinc electrode shape changes resulting from cell cycling have been studied. Experiments have been performed using zinc–silver oxide secondary cells of an industrial type. The results indicate that the extent of shape change is directly affected by the rate of discharge and charge, and the ZnO content of the electrolyte. The zinc electrode shape change can be mitigated by adding to the edge sections of the separator system a layer of non-woven fabric treated with $Fe(OH)_2$. The extent of shape change can also be reduced by increasing the separator thickness at the plate periphery. The orientation of the zinc electrode with respect to the earth's gravitational field (horizontally or vertically) on cycling, and the preparation methods for the zinc electrode (electrodeposition or slurry paste) have no apparent effect on the extent of zinc electrode shape change resulting from cell cycling.

1. Introduction

The alkaline silver–zinc and nickel–zinc secondary batteries are of considerable interest for applications where a high energy : weight ratio is desirable. However, a broader application of secondary batteries using zinc negatives has been restricted because of their limited cycle life. This is due mainly to the shape change of the zinc electrode. 'Shape change' refers to the redistribution of zinc active material over the zinc electrode surface and the reduction of the geometric area of the zinc electrode as a result of cell cycling.

A better understanding of the zinc electrode shape change is desirable not only because of the fundamental interest in the metal-deposition–dissolution reactions but also because of its technological importance in high energy density storage batteries.

The anodic behaviour of zinc in aqueous KOH solutions has been extensively studied by many investigators in recent years [1–19]. The oxidation product of the zinc electrode during the discharging cycle is highly soluble in strong alkali, forming $Zn(OH)_4^{2-}$ as the main product. During the subsequent charging cycle, the zincate deposits at the zinc electrode in a non-adherent dendritic form.

McBreen [20] has investigated the mechanism of zinc electrode shape change by monitoring the pattern of current and potential distribution over the surface of a zinc electrode during cycling. He has explained shape change in zinc electrodes in terms of non-uniform current distribution.

An improved zinc electrode, developed by Charkey [21] is based on a nucleation site concept for zinc. During discharge, a greater dissolution rate will occur at the electrode edges where a relatively large volume of electrolyte exists. On the subsequent charge, the zinc in solution tends to diffuse and redeposits on the high surface area portions of the electrode, i.e. the electrode centre, which, because of the structural arrangement in the cell, cannot be easily dissolved. This would cause shape change.

Newman *et al.* [22, 23] have developed a model for the zinc–silver oxide cell based on the hypothesis that the principal cause of shape change of zinc electrodes is zincate concentration changes together with convective flow, parallel to the apparent electrode surface, driven primarily by membrane pumping effects.

The purpose of this work was to examine the various factors which affect the shape change and to test different methods for the alleviation of such shape changes of zinc electrodes in a zinc–silver oxide cell.

2. Experimental

2.1. *Materials and chemicals*

The electrode grid material was 5Ag5-2/0 expanded silver screen, supplied by Exmet Corp. (Connecticut, USA)

The materials used for the preparation of the cell separator system consisted of Webril E 1452 non-woven polypropylene, supplied by Kendall Co. (Mass. USA); IC 40/100 radiation-grafted cellophane, supplied by RAI Corp., (New York); and S-950-CLS 2463 Viskon separator (rayon vinyon blend utilizing a cellulosic binder), supplied by Chicopee Co. (New Jersey).

Zinc oxide, mercuric oxide, mercuric chloride, silver peroxide, potassium hydroxide, polyvinyl alcohol (PVA), sodium carboxylmethyl cellulose (CMC), sodium hydroxide, hydrochloric acid, and all other chemicals used were of regeant grade. Dilute solutions were made with distilled water.

2.2. *Preparation of zinc electrodes*

Two methods, a slurry paste method and an electrodeposition method, were used to fabricate the zinc electrodes in order to observe the influence of the preparation method on the extent of electrode shape change.

2.2.1 Slurry paste method. About 6 g of electrode mixture (95 wt% ZnO + 2·0 wt% HgO + 2·0 wt% PVA + 1·0 wt% 30% KOH) was mixed with PVA solution. The paste was then applied to the grid of dimensions 6·4 x 6·0 cm cut from the expanded silver screen. After the grid was pasted, the plate was dried for about 4 hours. The plate was subsequently formed in a 5% KOH solution against a nickel dummy electrode at a rate of approximately 0·15 mA cm^{-2} for about 25 hours. After forming, the plate was thoroughly washed in distilled water to remove the KOH. The formed plate was pressed to the required plate thickness and then dried in an oven at about 55° C for a minimum time of 8 hours.

2.2.2. Electrodeposition method. The plating solution was prepared by adding 35·0 ± 0·5 g ZnO to each litre of 45% KOH solution, this being thoroughly stirred and equilibrated at 24–35° C. The grid section was placed in the acrylic frame, and the assembly was then immersed in the plating tank. Zinc was plated on the grid at a rate of approximately 0·15 A cm^{-2} of exposed grid area for about 45 hours. Two sheets of nickel screen, enveloped in acrylic frames, were used as the positive electrodes (anodes). After deposition, the plate was removed from the plating tank and washed in distilled water to remove the KOH. The plate was then treated in $HgCl_2$ solution. The plate was removed from the frame and pressed wet at 2000 lb after the $HgCl_2$ treatment, and then dried in an oven at 50–55° C for a minimum time of 4 hours.

2.3. *Preparation of silver oxide electrodes*

The silver oxide electrodes used for this study were prepared by a slurry paste method. 4 g of Ag_2O was made into a paste with about 1 ml of a 1% by weight aqueous solution of carboxylmethyl cellulose. The paste was then applied to the silver grid of dimensions 6·4 x 6·0 cm cut from the expanded silver screen. After drying at 70° C for about 2 hours, the plate was pressed at 45 000 lb.

2.4. *Test cell assembly*

A typical test cell assembly, as schematically shown in Fig. 1, comprised a negative zinc electrode, two silver oxide positive plates positioned to face each side of the zinc electrode with one nonconducting acrylic plate placed on each end of the electrode assembly to hold them in place. Nine such test cells were used in this study. The zinc electrodes used in Cells 1–8 were prepared by a slurry paste method while that used in Cell 9 was fabricated by an electrodeposition method for the purpose of observing the influence of the preparation method on the extent of zinc electrode shape change. In order to observe the influence of electrode orientation on the extent of shape change, the electrode plates of Cell 6 were purposely positioned horizontally instead of vertically as the electrode plates of all the other cells were positioned. The separator system inserted between the zinc and silver oxide electrodes in Cells 1, 2, 6, 7 and 8 consisted of one layer of Webril E 1452 non-woven polypropylene, three layers of RAI IC40/100 radiation-grafted cellophane, one layer

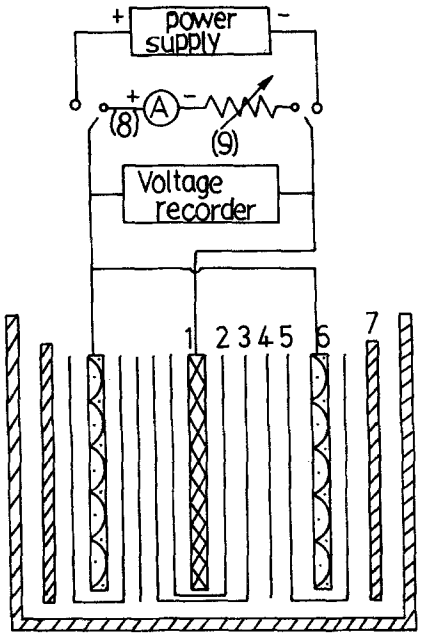

Fig. 1. Schematic diagram of a typical test cell assembly. 1. zinc electrode; 2. Webril E 1452 non-woven PP fabric; 3. three layers of RAI IC40/100 radiation-grafted cellophane; 4. no. 572 filter paper; 5. S-950-CLS 3463 Viskon separator; 6. silver oxide electrode; 7. acrylic plate; 8. Ammeter; 9. variable resistor.

of no. 572 filter paper, and one layer of S-950-CLS 3463 Viskon separator which was placed on the silver electrode side of the separator system. The 'special separator system' used in Cells 3 and 4 was modified by adding to its edge sections an additional layer (with dimensions shown in Fig. 2a) of Webril E 1452 non-woven polypropylene treated with $Fe(OH)_2$. In addition to the non-woven fabric, the filter paper, and the Viskon separator, the separator system of Cell 5 consisted of five layers of RAI cellophane, three of which were cut with the central section removed having dimensions shown in Fig. 2b.

After inspection, the electrode assembly was installed in the rectangular acrylic case filled with electrolyte.

2.5. *Experimental procedure*

After the test cell was filled with 60 ml of electrolyte (40% KOH + 30 mg ZnO/ml KOH for Cell 8; 40% KOH + 60 mg ZnO/ml KOH for all other cells) and soaked for 24 hours, the cycling test was started. The nine cells were divided into three groups according to the depth and conditions of charge and discharge. Group 1 cells (comprising Cells 1 and 3) were discharged at 1·0 A for 45 min and were charged at 0·5 A to a cell voltage of 2·10 V. Group 2 cells (comprising Cells 2, 4, 5, 6, 8 and 9) were discharged at 2·0 A for 23 min, and were charged at 1·0 A to 2·10 V. Group 3 (comprising only Cell 7) was discharged at 2·0 A for 31 min and was charged at 1·0 A to 2·10 V.

The cells were discharged through a series of variable resistors. Discharge curves were displayed using one Gould Brush 220 and two Linear Model 232 recorders. Constant currents and potentials were supplied by conventional regulated power supplies.

After 61 cycles the zinc electrode was removed from the test cell assembly in the charged condition and was examined for the general patterns of shape change using a Cambridge JSU-3 scanning electron microscope. The zinc electrode was then washed thoroughly with distilled water to remove the electrolyte. After drying in an oven at about 50° C, the zinc electrode was cut into nine sections of equal size (2·0 x 2·0 cm) which were marked according to their relative positions designated Sections 1–9 (as shown, for example, in Fig. 3). The thickness and weight of each section of the zinc electrode were then measured carefully to

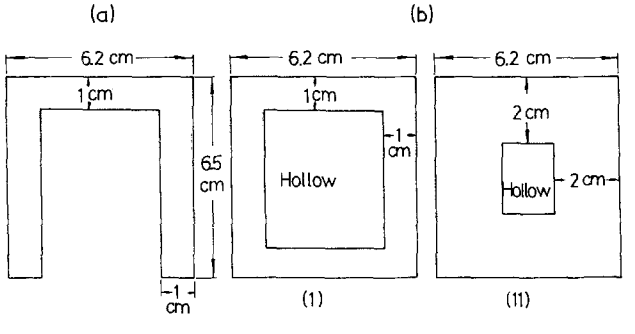

Fig. 2. (a) Dimensions of the Webril E1452 non-woven PP films added to the separator systems of Cells 3 and 4.
(b) Dimensions of the RAI IC40/100 radiation grafted cellophane membrane added to the separator systems of Cell 5. Two layers of (i) and one layer of (ii).

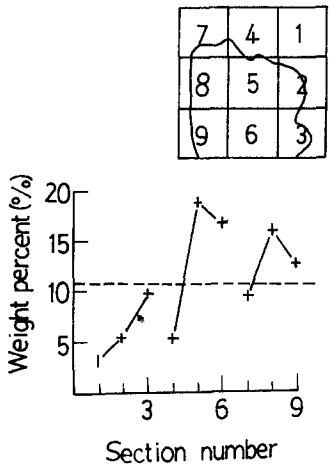

Fig. 3. The electrode shape change pattern and the weight per cent versus section number plot for the zinc electrode of Cell 1 after cycling.

obtain accurate quantitative data of electrode shape change.

2.6. *Scanning electron micrographs*

In order to investigate the influence of the fabrication method used for the zinc electrode on the extent of shape change, the surface structures of the zinc electrodes prepared by the slurry paste method and those prepared by the electrodeposition method were also investigated with a scanning electron microscope (Cambridge JSU-3) before and after cycling tests, and SEM photographs taken for detailed examination.

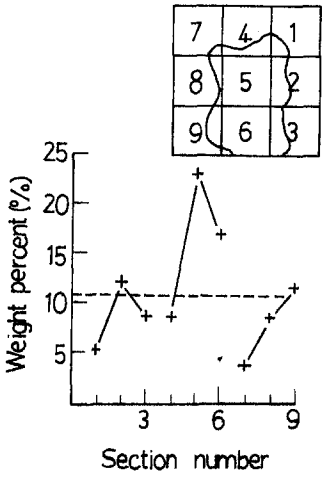

Fig. 4. The electrode shape change pattern and the weight per cent versus section number plot for the zinc electrode of Cell 2 after cycling.

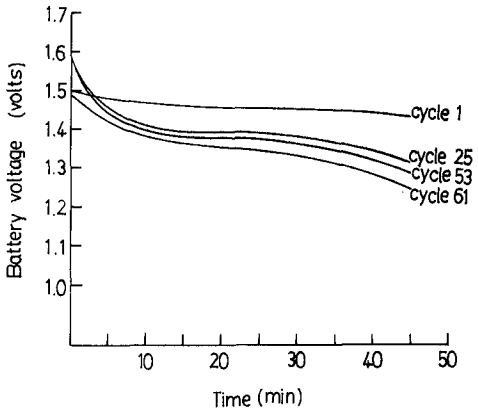

Fig. 5. Discharge performance curves of Cell 1 at four different stages of cell cycling.

3. Results and discussion

After cycling, the change of the weight per cent values for different sections of a zinc plate from their average value (one ninth of the total weight of a zinc plate) before cycling gives a quantitative measure of the redistribution of zinc active material over the zinc plate surface and thus shows the trend of the zinc electrode shape change.

From the data obtained for the nine test cells, it was observed that, for nearly every zinc electrode of the nine test cells studied, the central section (Section 5) had the highest weight per cent value of all the nine sections of each plate. These data show that, in general, the zinc active material agglomerated towards the central part of the zinc plate surface after cycling.

Figs. 3, 4, 7, 8 and Figs. 11–15 present the zinc

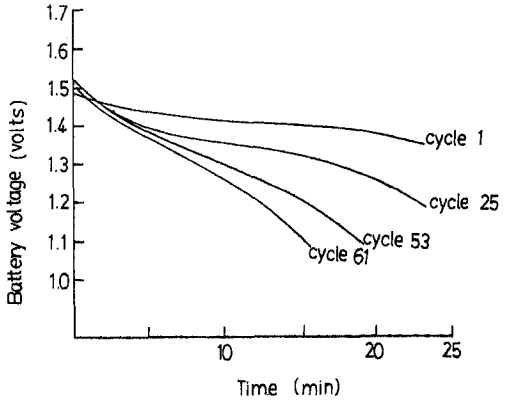

Fig. 6. Discharge performance curves of Cell 2 at four different stages of cell cycling.

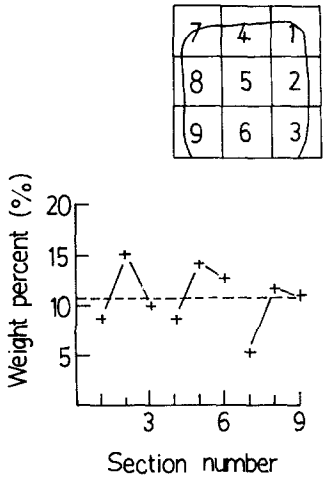

Fig. 7. The electrode shape change pattern and the weight per cent versus section number plot for the zinc electrode of Cell 3 after cycling.

active material redistribution by weight per cent value versus section number plots together with sketches of the shape change pattern after 61 cycles. These shape change patterns were sketched according to the observed shape change on the surfaces of the zinc electrodes of Cells 1–9. The areas inside the boundary curves indicate where the zinc active material has agglomerated; the thickness of these areas increased by as much as a factor of nearly three in some places (the original thickness of the uncycled zinc plates was about 0·40 ± 0·04 mm; the thickness of the areas inside the boundary curves increased to 0·40–1·10 mm after cycling). The areas between the boundary curves and the plate edges were nearly denuded of zinc active material and the thickness of these areas decreased to that of the unpasted grid (0·22 mm) in some places.

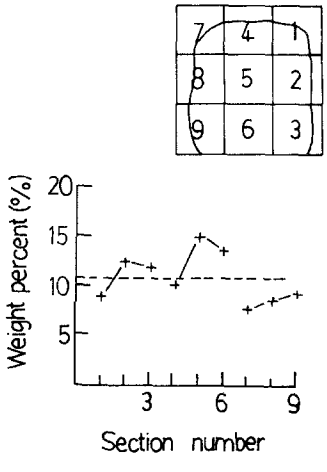

Fig. 8. The electrode shape change pattern and the weight per cent versus section number plot for the zinc electrode of Cell 4 after cycling.

In each of the weight per cent value versus section number plots, the horizontal broken line represents the average weight per cent value of all the sections of the zinc plate before cycling. The solid discontinuous curve represents the weight per cent values of different sections of the zinc plate after 61 cycles of cycling.

3.1. *Effect of charge and discharge rate*

Fig. 3 shows the results of the redistribution of zinc material over the zinc electrode surface of Cell 1 after 61 cycles (discharged at 1·0 A for 45 min, charged at 0·4 A to 2·10 V). It can be observed that little active material remained in Sections 1, 2 and 4, and considerable gain in zinc deposit thickness occurred in Sections 5, 6 and 8.

Fig. 4 shows the shape change pattern of the zinc electrode of Cell 2 after 61 cycles (discharged at 2·0 A for 23 min, charged at 1·0 A to 2·1 V). Comparing Fig. 4 with Fig. 3, the experimental results reveal that the zinc electrode of Cell 2 underwent a much greater loss of effective geometric area than that of Cell 1. It also shows that the thickness of the central part of the zinc plate of Cell 2 increased much more than that of Cell 1. Therefore, these results indicate clearly that the extent of zinc electrode shape change increases with the increasing of charge and discharge rate applied to the cell.

Figs. 5 and 6 show the discharge curves at Cycles 1, 25, 53 and 61 for Cell 1 and Cell 2 respectively. It can be observed from these two figures that the discharge performance of Cell 1 was much better than that of Cell 2, especially at the later stages of cell cycling.

3.2. *Effect of separator system modification*

Figs. 7 and 8 present the patterns of shape change of the zinc electrodes of Cells 3 and 4, respectively. Cell 3 was cycled under the same conditions (charged and discharged at the same rate and to the same cut-off terminal conditions) as those applied to Cell 1. It can be noted from Fig. 7 that

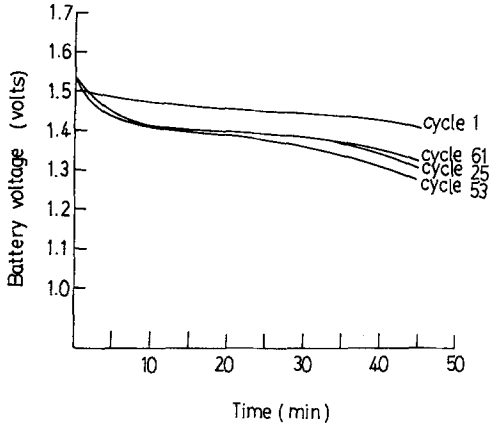

Fig. 9. Discharge performance curves of Cell 3 at four different stages of cell cycling.

the extent of the zinc electrode shape change of Cell 3 was less than that of Cell 1 (as shown in Fig. 3), and the loss of effective geometric area of the zinc plate of Cell 3 was much reduced. Cell 4 was cycled under the same conditions as those applied to Cell 2. From the electrode shape change data presented in Figs. 4 and 8, it can be observed that the extent of shape change of the zinc electrode of Cell 4 after cycling was also less than that occurring on the zinc electrode of Cell 2. Therefore, the experimental results presented in Figs. 7 and 8 show clearly that, by using the 'special separator system', the extent of zinc electrode shape change was effectively reduced.

The addition of a layer of non-woven fabric treated with $Fe(OH)_2$ [in effect, it is likely to be $Fe_2O_3xH_2O$ since $Fe(OH)_2$ is readily oxidized by atmospheric oxygen] to the edge sections of the separator system has the effect of both lowering the hydrogen overpotential and reducing the plating efficiency of the zinc material on the edge sections of zinc electrode; besides, the soluble iron species in the electrolyte can affect the morphology of the zinc electrode. These effects will depress the zinc deposition on the edge sections and thus will improve the uniformity of the distribution of zinc materials on the electrode plate surface in the early stages of cycling; consequently, the initiation of the electrode shape change will be delayed. This is in accordance with the test results obtained from test Cells 3 and 4, that the shape change occurred more slowly and the extent of shape change was reduced sharply when such a layer of non-woven fabric was added to the separator system.

Figs. 9 and 10 present the discharge curves at Cycles 1, 25, 53 and 61 for Cell 3 and Cell 4, respectively. After comparing the discharge curves presented in Figs. 9 and 10 with those presented in Figs. 5 and 6, it should be apparent that the discharge performances of Cells 3 and 4 were significantly improved over those of Cells 1 and 2, respectively.

The separator system of the zinc electrode used in Cell 5 comprised five layers of IC 40/100 radiation-grafted cellophane membrane (see Fig. 2b) instead of only three layers as used in other cells. Fig. 11 shows the pattern of zinc electrode

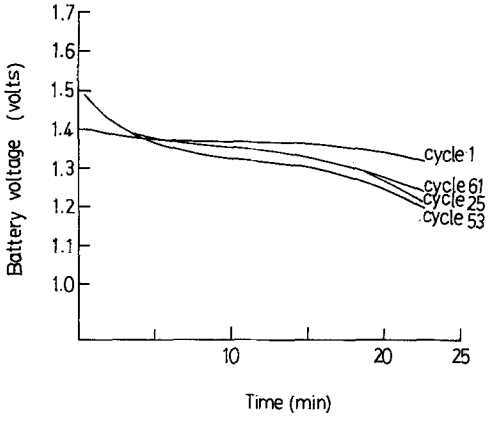

Fig. 10. Discharge performance curves of Cell 4 at four different stages of cell cycling.

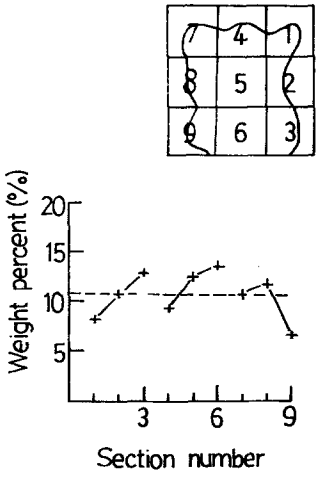

Fig. 11. The electrode shape change pattern and the weight per cent versus section number plot for the zinc electrode of Cell 5 after cycling.

shape change for Cell 5 after cycling (cycled under the same conditions as those applied to Cell 2). From the data summarized in Fig. 11, it should be apparent that the extent of zinc electrode shape change was greatly reduced in comparison with that of Cell 2 (as shown in Fig. 4).

Increasing the thickness of the edge sections of the separator system has the effect of modifying the zincate diffusion profiles and reducing the local conductivity of the electrolyte at the electrode edges. These effects can reduce the primary current distribution at the plate edges and thus reduce the non-uniformity of metal deposition on the electrode surface at the beginning of cycling which results in the subsequent onset of electrode shape change. This is because, in a cell with plane parallel electrodes, the primary current density is highest at the edges of the electrodes since the current can flow through the solution beyond the edges of the electrodes [24, 25]. This non-uniformity of primary current distribution causes the subsequent differences in polarizability over the electrode surface and the onset of electrode shape change. The improvement achieved on the extent of zinc electrode shape change of Cell 5 may be explained by this reasoning.

3.3. *Effect of orientation of zinc electrodes during cycling*

Cell 6 was operated by lying the electrode assembly in a horizontal position instead of in a vertical position as the other cells were operated. The cell was discharged and charged at the same rate and to the same cut-off terminal conditions as those of Cell 2. Fig. 12 presents the resulting shape change pattern of the zinc electrode of Cell 6 after cycling. It can be noticed that the zinc material agglomerated toward the central region of the electrode surface. It is also shown that in this case the lower edge of the zinc plate was deprived of zinc material, and by this it differs from the shape change patterns resulting in other zinc electrodes which were vertically positioned on cycling. However, the effect of this difference on the discharge performance of zinc electrodes is insignificant as can be observed from the discharge curves. This is an indication that the gravity effect is unimportant with respect to electrode shape change. This conclusion is in agreement with the observations of McBreen [20].

3.4. *Effect of the depth of discharge*

Cell 7 was cycled by discharging it at 2·0 A for 31 min and charging it at 1·0 A to 2·10 V. It was discharged deeper than Cell 2. Fig. 13 shows the shape change pattern of the zinc electrode of Cell 7 after cycling. It can be observed from this figure that the extent of zinc electrode shape change of this cell was greater than that of the zinc electrode of Cell 2. This result indicates that the extent of electrode shape change is directly related to the depth of electrode discharge.

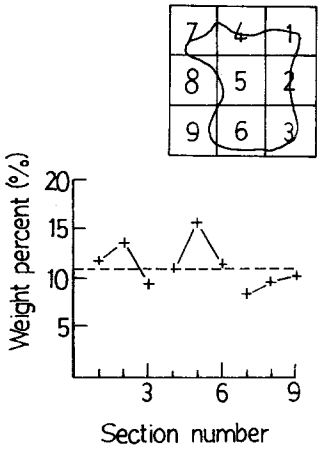

Fig. 12. The electrode shape change pattern and the weight per cent versus section number plot for the zinc electrode of Cell 6 after cycling.

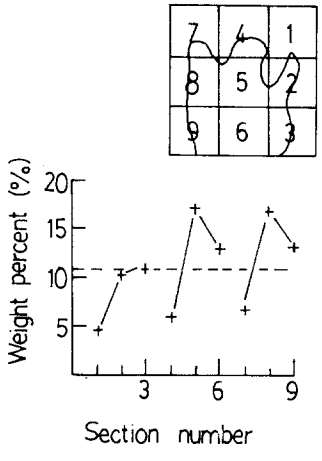

Fig. 13. The electrode shape change pattern and the weight per cent versus section number plot for the zinc electrode of Cell 7 after cycling.

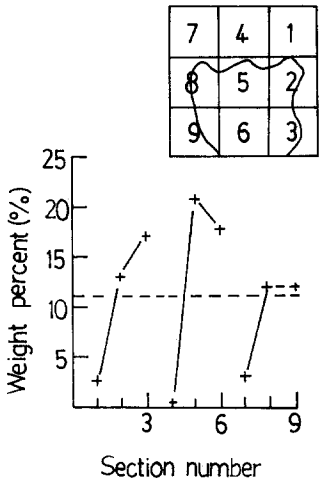

Fig. 14. The electrode shape change pattern and the weight per cent versus section number plot for the zinc electrode of Cell 8 after cycling.

3.5. *Effect of the ZnO content of electrolytes*

The ZnO content of the electrolyte in Cell 8 was 30 mg of ZnO per ml of 40% KOH, whilst that in the other test cells was 60 mg of ZnO per ml of 40% KOH. Cell 8 was cycled under the same conditions as those applied to Cell 2. Fig. 14 shows the resulting shape change pattern of the zinc electrode of this cell after cycling. It is shown that Sections 1, 4 and 7 were nearly denuded of zinc materials, and most of the zinc agglomerated toward Sections 3, 5 and 6.

In a secondary zinc cell, the addition of ZnO to the electrolyte of 40% KOH has the advantage of reducing the loss by anodic dissolution and increasing the cycle life of the cell. Zinc species react with OH^- ions of the electrolyte to form various soluble zincate complexes, mainly $Zn(OH)_4^{-2}$, during discharge. When the ZnO content is low, the zincate complex formed during discharge can easily diffuse into the solution. This promotes the reaction and reduces the polarizability, hence the reaction rate at the edges of electrodes will increase greatly because the current distribution on the electrode surface approaches the primary current distribution. On the subsequent charging, the zincate at the plate periphery tends to diffuse and deposit back on the central part of the zinc plate due to the zincate concentration gradient formed between the edge and centre of the electrode. The transfer of zincate toward the centre of the electrode together with the loss of soluble zinc species from the plate periphery results in an electrode shape change.

3.6. *Effect of fabrication method for zinc electrodes*

In this study the zinc electrode of Cell 9 was prepared by the electrodeposition method, while the electrodes of all other test cells were prepared by the slurry paste method. Cell 9 was cycled under the same conditions as those of Cell 1. Fig. 15 shows the resulting shape change of the zinc electrode of this cell after cycling. A comparison between Fig. 15 and Fig. 3 indicates that the extent of shape change is comparable for Cells 9 and 1.

Fig. 16a and b show scanning electron microscope (SEM) photographs of the surface structure of the uncycled zinc electrode of Cell 9. They show clear crystalline patterns resembling veins on tree leaves. Figs. 17a and b show SEM pictures of the surface structure of the uncycled zinc electrode of Cell 1, which was prepared by the slurry paste method. It can be seen that the surface has an irregular mossy appearance. Figs. 18 and 19 show SEM photographs of the surface structures of cycling-tested zinc electrodes of Cell 9 and Cell 1, respectively. Comparing Fig. 18 with Fig. 19, it can be seen clearly that the appearances of the two

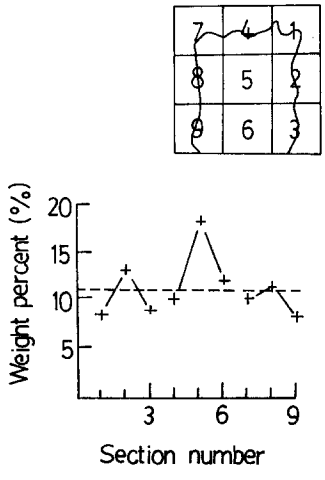

Fig. 15. The electrode shape change pattern and the weight per cent versus section number plot for the zinc electrode of Cell 9 after cycling.

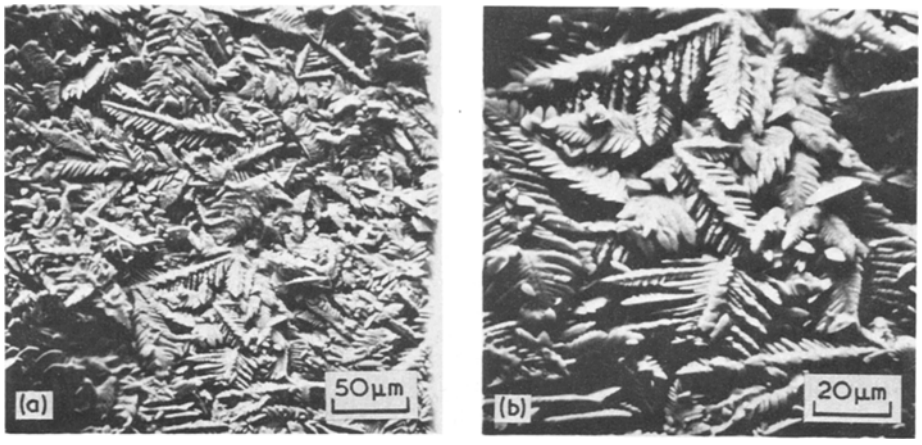

Fig. 16. Scanning electron micrographs of the surface structure of an uncycled zinc electrode fabricated by the electrodeposition method. Magnification: (a) × 300 (b) × 750.

zinc electrode surfaces became similar after cycling.

The results of SEM observations and cycling tests indicate that under the same cycling test conditions, the zinc electrode fabricated by the electrodeposition method showed the same degree of shape change as that occurring in the electrodes fabricated by the slurry paste method.

4. Conclusions

The following conclusions were reached.

(a) The data from this investigation demonstrate that the extent of zinc electrode shape change in a secondary battery is directly affected by the charge and discharge rate of the cell.

(b) The addition to the edge sections of the zinc electrode of a separator system consisting of a layer of non-woven fabric treated with $Fe(OH)_2$ has the effect of lowering the hydrogen overpotential and reducing the zinc plating efficiency on the edge sections of zinc electrodes. These effects can delay the initiation of electrode shape change, and thus can effectively mitigate the extent of electrode shape change.

(c) Increasing the thickness of the edge sections of the electrode separator system can reduce the non-uniformity of current distribution and zinc

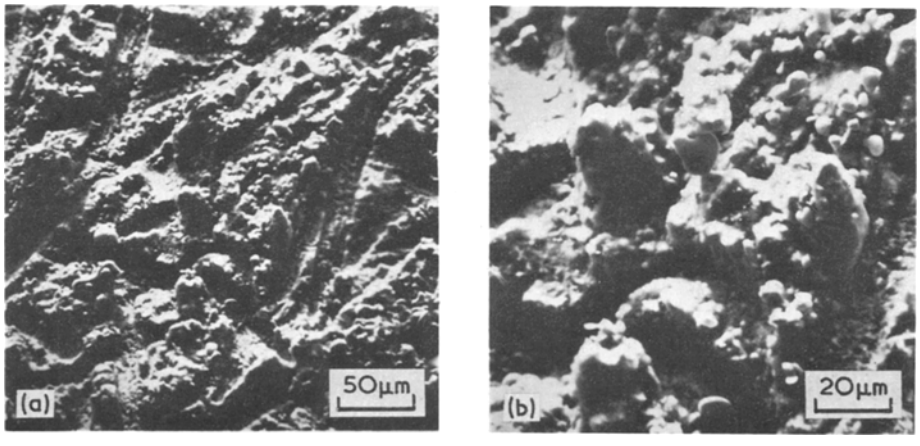

Fig. 17. Scanning electron micrographs of the surface structure of an uncycled zinc electrode fabricated by the slurry paste method. Magnification: (a) × 300, (b) × 750.

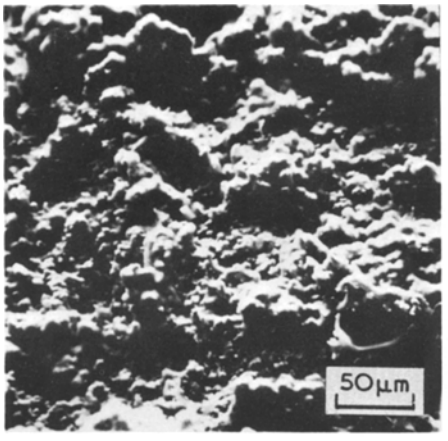

Fig. 18. Scanning electron micrograph of the surface structure of a zinc electrode fabricated by the electrodeposition method, after 61 cycles of cycling in Cell 9. Magnification: × 300.

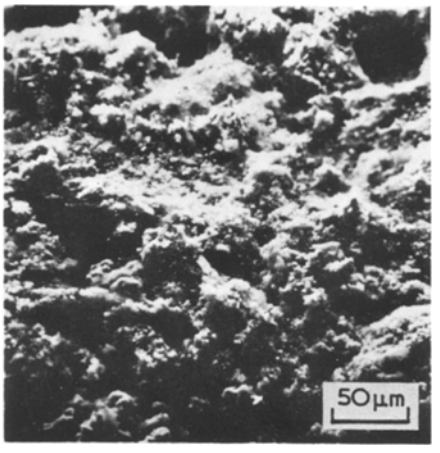

Fig. 19. Scanning electron micrograph of the surface structure of a zinc electrode fabricated by the slurry paste method, after 61 cycles of cycling in Cell 2. Magnification: × 300.

material redistribution at the beginning of cell cycling, and thus the extent of electrode shape change can be effectively restrained.

(d) During the cell cycling operation, the effect of the orientation of the zinc electrode (horizontally or vertically with respect to the earth's gravitational field) on the extent of electrode shape change is insignificant.

(e) The addition of ZnO to the electrolyte of 40% KOH in the test cells has the effect of reducing loss by anodic dissolution and increasing the cycle life of the battery.

(f) Under the same cycling test conditions, the electrode prepared by the electrodeposition method showed the same degree of shape change as that occurring in the electrodes prepared by the slurry paste method.

Acknowledgement

The work was carried out with the financial assistance of the National Science Council of the Republic of China.

References

[1] T. P. Dirkse, D. De Wit and R. Shoemaker, *J. Electrochem. Soc.* **115** (1968) 442.
[2] S. Arouete, K. F. Blurton and H. G. Oswin, *ibid* **116** (1969) 166.
[3] J. W. Diggle, A. R. Despic and J. O'M. Bockris, *ibid* **116** (1969) 1503.
[4] M. N. Hull, J. E. Ellison and J. E. Toni, *ibid* **117** (1970) 192.
[5] J. O'M. Bockris, Z. Nagy and A. Damjanovic, *ibid* **119** (1972) 285.
[6] J. W. Diggle and A. Damjanovic, *ibid* **119** (1972) 1649.
[7] A. R. Despic and M. M. Purenovic, *ibid* **121** (1974) 121.
[8] W. Van Doorne and T. P. Dirkse, *ibid* **122** (1975) 1.
[9] T. S. Lee, *ibid* **122** (1975) 171.
[10] P. F. Hutchinson and J. Turner, *ibid* **123** (1976) 183.
[11] T. P. Dirkse and N. A. Hampson, *Electrochim. Acta* **16** (1971) 2049.
[12] *Idem*, *ibid* **17** (1972) 135.
[13] *Idem*, *ibid* **17** (1972) 387.
[14] *Idem*, *ibid* **17** (1972) 813.
[15] *Idem*, *ibid* **17** (1972) 1113.
[16] A. R. Despic, Dj. Jovanovic, and T. Rakic, *ibid* **21** (1976) 63.
[17] R. N. Elsdale, N. A. Hampson, P. C. Jones and A. N. Strachan, *J. Appl. Electrochem.* **1** (1971) 213.
[18] G. Coates, N. A. Hampson, A. Marshall and D. F. Porter, *ibid* **4** (1974) 75.
[19] R. W. Lewis and J. Turner, *ibid* **5** (1975) 343.
[20] J. McBreen, *J. Electrochem. Soc.* **119** (1972) 1620.
[21] A. Charkey, 'Advances in Component Technology for Ni–Zn Cells', Energy Research Corporation, Danbury, Connecticut (1976).
[22] K. W. Choi, D. N. Bennion and J. Newman, *J. Electrochem. Soc.* **123** (1976) 1616.
[23] K. W. Choi, D. Hamby, D. N. Bennion and J. Newman, *ibid* **123** (1976) 1628.
[24] J. S. Newman, 'Electrochemical Systems', Prentice-Hall Inc., Englewood Cliffs, New Jersey (1973) p. 241.
[25] C. Wagner, *J. Electrochem. Soc.* **98** (1951) 116.